NIH Public Access
Author Manuscript
J Biomech. Author manuscript; available in PMC 2015 June 27.

Published in final edited form as:
J Biomech. 2014 June 27; 47(9): 2102–2114. doi:10.1016/j.jbiomech.2013.10.059.

Biomechanical adaptation of the bone-periodontal ligament (PDL)-tooth fibrous joint as a consequence of disease

Jeremy D. Lin[a], **Jihyun Lee**[a], **Hüseyin Özcoban**[b], **Gerold A. Schneider**[b], and **Sunita P. Ho**[a,*]

[a]Division of Biomaterials and Bioengineering, Department of Preventive and Restorative Dental Sciences, School of Dentistry, University of California San Francisco, CA 94143

[b]Institute of Advanced Ceramics, Hamburg University of Technology, Hamburg, Germany

Abstract

In this study, an *in vivo* ligature-induced periodontitis rat model was used to investigate temporal changes to the solid and fluid phases of the joint by correlating shifts in joint biomechanics to adaptive changes in soft and hard tissue morphology, and functional space. After 6 and 12 weeks of ligation, coronal regions showed a significant decrease in alveolar crest height, increased expression of TNF-α, and degradation of attachment fibers as indicated by decreased collagen birefringence. Cyclical compression to peak loads of 5-15N at speeds of 0.2-2.0N/mm followed by load relaxation tests showed decreased stiffness and load rate values, load relaxation, and load recoverability, of ligated joints. Shifts in joint stiffness and reactionary load rate increased with time while shifts in joint relaxation and recoverability decreased between control and ligated groups, complementing measurements of increased tooth displacement as evaluated through digital image correlation. Shifts in functional space between control and ligated joints were significantly increased at the interradicular (Δ10-25μm) and distal coronal (Δ20-45μm) regions. Histology revealed time-dependent increases in nuclei elongation within PDL cells and collagen fiber alignment, uncrimping, and directionality, in 12-week ligated joints compared to random orientation in 6-week ligated joints and to controls. We propose that altered strains from tooth hypermobility could cause varying degrees of solid-to-fluid compaction, alter dampening characteristics of the joint, and potentiate increased adaptation at the risk of joint failure.

1. Introduction

During function, the tooth is subjected to micromotion that prompts homeostasis – a vital state that sustains the fundamental nature of the bone-periodontal ligament (PDL)-cementum

*corresponding author: Phone: 415-514-2818. sunita.ho@ucsf.edu.

Coauthor contribution is as follows: Study design (JDL, SPH), study conduct (JDL, JL), data collection (JDL, JL), data analysis (JDL, JL, HO, SPH), data interpretation (JDL, JL, SPH), drafting of the manuscript (JDL, SPH), revising manuscript content (JDL, GS, SPH), approving final version of manuscript (JDL, JL, HO, GS, SPH), responsibility for the integrity of data analysis (JDL, JL, HO, GS, SPH).

Conflict of Interest Statement: We acknowledge that all authors do not have any conflict of interest and were fully involved in the study and preparation of the manuscript.

Publisher's Disclaimer: This is a PDF file of an unedited manuscript that has been accepted for publication. As a service to our customers we are providing this early version of the manuscript. The manuscript will undergo copyediting, typesetting, and review of the resulting proof before it is published in its final citable form. Please note that during the production process errors may be discovered which could affect the content, and all legal disclaimers that apply to the journal pertain.

NIH-PA Author Manuscript
NIH-PA Author Manuscript
NIH-PA Author Manuscript

NIH-PA Author Manuscript

NIH-PA Author Manuscript

NIH-PA Author Manuscript

complex by absorbing and transmitting mechanical loads through various soft and hard structural elements (Beertsen et al., 1997; Herring, 2012; Ten Cate, 1998). Homeostasis is due to an orchestration of events at several hierarchical length scales that include cells, tissues *per se*, interfaces between tissues, and eventually the entire organ (Bartold, 2012; Beertsen et al., 1997). Hence, the optimum contributions of elastic and time-related viscous response are maintained, allowing joint recovery upon removal of functional forces. However, a shift in homeostasis can cause modeling of the soft and hard structural elements (Giannobile et al., 2003), subsequently leading to an overall disturbance in organ biomechanics (Lee and Lin et al., 2013). Such shifts are often a result of perturbations (periodontal disease, parafunctional loads, and therapeutic load) to physiologic tooth mobility, which over prolonged loading can cause abnormal tooth displacement within the alveolar socket (Hurng et al., 2011).

Shifts in joint biomechanics can be sensed by both softer and harder tissues due to the “mechanoresponsive” nature of respective cellular components (Ingber, 2003, 2005). As a result, the shifts in mechanical signals (within normal and/or perturbed conditions) could prompt varying intensities and localization of biomolecules, which in turn could redefine the homeostatic nature of the complex (Ingber, 2006). Knowledge about the altered mechanoresponse of a joint is essential because within most mammals, the cyclic function (mastication) causes the joint to react as a result of the combined effect of constitutive properties from soft and hard tissues and an overall shift in strain patterning within the joint (Carter and Beaupré, 2001; Chen and Ingber, 1999). Components in softer viscoelastic PDL include the solid phase of the organic matrix and the fluid phase of interstitial fluid and blood (Bergomi et al., 2010). When broken down to the molecular constituents, the solid phase can be further analyzed for changes in macromolecular structures of collagen and semi-solid proteoglycans (PGs) and breakdown of the interconnecting network between collagen and PG, while the fluid phase can be affected by bound and unbound water. Such changes in constituitive properties can be compounded by inflammation related changes in hemodynamics, pH, and temperature (Giannobile et al., 2003; Holmes et al., 1985; Kinney et al., 2007). Together, the change in concentration, type, and interaction of constituents affects the overall time related response, i.e. the viscous nature of the fibrous joint that can be mapped by mimicking varied loading rates (speed of loading) (Alexopoulos et al., 2005; Duenwald et al., 2009, 2010; Guilak et al., 1994; Mow et al., 1984). Alterations to each of the constitutive properties of harder and softer elements in a fibrous joint can occur through disease and/or pathological loading, thereby decreasing the ability of the joint to optimally respond to function. Resulting changes in strain patterns can shift the organ into compensatory function, which can also be identified through changes in form (Carter and Beaupré, 2001; Ingber, 2003).

In this study, the induced perturbation to the complex of a small-scale animal model is the globally prevalent periodontitis, which is known to affect tooth biomechanics (Dasanayake, 2010; Doyle and Bartold, 2012; Lee and Lin et al., 2013). Inflammatory macromolecules during disease onset and progression cause degradation of softer structural elements such as collagen and PGs, breakdown of the organic network, resorption and alteration of mineral composition and content, and changes in fluid flux and water retention characteristics.

NIH-PA Author Manuscript

NIH-PA Author Manuscript

NIH-PA Author Manuscript

Without clinical intervention, the amount of attachment between tooth and bone decreases and with persistent disease increases tooth mobility within the bony socket. Our previous study illustrated an early-stage mechanobiological effect of the joint due to increased tooth mobility from periodontitis (Lee and Lin et al., 2013). With the increased expression of mechanosensitive proteins under perpetuating function, the joint was postulated to have an altered biomechanical response through amplified and/or decreased strains. Hence, it is proposed that prolonged functional loads in the presence of disease-induced inflammation at the originally strain-amplified hot spots accelerate joint degeneration through mechanobiological adaptation. The objective is to correlate changes in load-displacement response coupled with *in situ* imaging to histology to detect such adaptations due to disease progression.

2. Materials and Methods

Please refer to the supplemental information for details on the ligature model setup and specimen preparation for *in situ* loading. In brief, 4-0 silk suture threads soaked in 7.1mg of lipopolysaccharide (LPS) from *Escherichia coli* serotype 055:B5 (Sigma-Aldrich, St. Louis, MO, L2880) per 1mL of 1× Tris-buffered saline (TBS, pH7.4) were placed in the experimental group (N=5 for each time point of 6 and 12weeks of ligation) to induce periodontitis in 6-week-old male Sprague Dawley rats (Lee and Lin et al., 2013). Rats belonging to the control group (N=5 for each time point) were flossed with 4-0 silk ligatures without LPS.

2.1. Uniaxial compression tests

Biomechanical testing of experimental and control groups was performed by cyclically loading the second maxillary molar at various displacement rates of 0.2, 0.5, 1.0, 1.5, and 2.0mm/min, to tease out the contributions of the various constitutive properties within the joint (Hiiemae, 2004; Lin et al., 2013; Thomas and Peyton, 1983). Loading was performed until peak reactionary load responses of 5, 7, 10 and 15N (Nies and Ro, 2004), were detected by the transducer. Initial contact was ensured through detection of a response load of 0.2N. The sequence of permutations was a set of increasing magnitudes of displacement rate per increasing peak load. All cycles were brought back to the initial baseline load of 0.2N. Specimens were loaded 4 times to each peak load at different displacement rate combinations, and only the last 3 cycles were used for various analyses. Data was collected at a sampling time of 100ms. Recovery and rehydration of periodontal tissues between each cycle were allowed through a one minute wait period.

2.2. Load relaxation tests

Load relaxation studies were performed on the same second maxillary molars as described in 2.1. Molars were loaded at displacement rates of 0.2, 1.0, and 2.0mm/min, to peak reactionary loads of 5, 10, and 15N. After the desired peak reactionary load was reached for each permutation, the jaws of the testing device were held in place for two minutes. Unloading of the molar was then performed, and specimens were allowed two minutes for recovery and rehydration of periodontal tissues before biomechanical testing using the next permutation parameters was performed.

NIH-PA Author Manuscript

NIH-PA Author Manuscript

NIH-PA Author Manuscript

2.3. Analyses

Stiffness (N/mm) and the reactionary load rate (N/s) were determined by using a linear regression model fit to the last 30% of the load-displacement and load-time data, respectively, of each compression cycle (Fung, 1993; Lin et al., 2013; Popowics et al., 2009). The two minute hold portions of the load-time profiles were compared to evaluate load relaxation. The first 30% percent of data points in the unloading curves were used to generate unloading load rate responses, i.e. load recovery between control and ligated joints.

3. Results

3.1. Response to uniaxial loads

Ligated joints exhibited a decreased reactionary load rate (also known as reactionary response) (Figs.1a,b), a decreased stiffness, and an increased displacement compared to controls at both time points (Figs.1c,d). Additionally, the reactionary load rate diverged with increasing speeds for both control and ligated joints. A shift in reactionary load rate and joint stiffness over time was observed by identifying changes in slope of the linear fits to control and ligated data sets between the 6-week and 12-week time points (Figs.1e,f). With the exception at 5N of peak load, the magnitude of slope differences in load rate at the 12-week time point were greater than slope differences at the 6-week time point. These observed differences increased with increasing peak loads (Fig.1e). With the exception at 1.5mm/min, stiffness slope differences at the 12-week time point were greater than slope differences at the 6-week time point (Fig.1f). Unlike slope differences in load rate, no significant trends were observed in stiffness shifts across displacement rates. However, the 12-week ligated specimens demonstrated a higher shift in stiffness from control compared to 6-week ligated specimens.

3.2. Load relaxation and recovery characteristics

A nonlinear load relaxation response over a hold phase of 2min (Fig. 2a) at 5, 10, and 15N, of reactionary peak loads at a slower speed of 0.2mm/min (Figs. 2b,d) was observed. In comparison, loading to the same peak loads but at a faster speed of 2mm/min (Figs.2c,e) demonstrated a linear load relaxation response. Control joints appeared to have a greater range of load relaxation than diseased joints. At 6 weeks, the ligated joint exhibited decreased load relaxation compared to the control joint when loaded at 0.2mm/min (Fig.2b). Similar behavior but to a lesser extent was observed when the displacement rate was increased by tenfold (Fig.2c) and after 12weeks (Fig.2d,e). Both control and ligated joints at 12weeks exhibited less load relaxation compared to those at 6 weeks.

During recovery of the joint for the same drop in load (Fig.3a), rapidly unloaded specimens (Figs.3c,e,g) demonstrated a nonlinear effect within the first 2s of unloading compared to the slowly unloaded (Figs.3b,d,f and corresponding insets) specimens. Ligated joints at 6weeks exhibited overall decreased load recovery compared to controls at 0.2 and 2.0mm/min (Figs.3b,c). The diseased joints took less time to recover compared to healthy joints at 0.2 and 2.0mm/min of unloading regardless of reactionary peak load (Fig.3f,g). At 12weeks, ligated joints exhibited greater ranges but similar load recovery characteristics compared to control joints at 0.2mm/min and 2.0mm/min (Fig.3d,e) for all peak loads. The

NIH-PA Author Manuscript

NIH-PA Author Manuscript

NIH-PA Author Manuscript

ligated joints displayed similar slopes to controls at 0.2mm/min and 2.0mm/min of unloading (Fig.3f,g).

3.3. Tooth displacement using digital image correlation (DIC)

At 12weeks, the control second molar exhibited minimal horizontal displacement (Fig.4a) with a predominantly vertical depression (40-50μm, Fig.4b) towards the alveolar bone. In comparison to controls, the molar within the ligated joint exhibited increased horizontal displacement towards the mesial direction (Fig.4c). This displacement gradually increased from the crown (10-15μm) down in the coronal (20-30μm) and apical (30-35μm) regions of the roots. Ligated molars also demonstrated increased vertical depression (65-85μm) into the alveolar socket (Fig.4d) compared to control joints.

3.4. Morphological differences in PDL-space

The PDL-space at the interradicular and distal apical regions increased significantly at 6 and 12weeks when compared to corresponding regions in controls, while the PDL-space illustrated decreasing trends all along the mesial and the distal coronal regions (Fig.5a). While the interradicular PDL-space increased between 6 and 12 weeks, the PDL-space of the distal apical region decreased. Differences between control and ligated PDL-spaces in both of these regions showed net positive differences (average ligated joints had greater PDL-spaces than corresponding average control joints), while mesial coronal, mesial apical, and distal coronal regions, all exhibited net negative differences (average control joints had greater PDL-spaces than corresponding average ligated joints).

3.5. Histological comparisons

3.5.1. Osteoclastic activity—At 6weeks, the PDL-bone interfaces at mesial furcation (Figs.5b.ii,vi) and distal (Figs.5b.iv,vii) regions of ligated exhibited increased expression of TRAP(+)-stained osteoclasts and reversal lines, especially in apical regions of bone opposite to secondary cementum. Furthermore, clear layers of outgrowth that were devoid of cementocytes and entered into the PDL space were observed in mesial furcation regions and in greater widths in distal regions within the ligated joint compared to controls. At 12weeks (Figs.5b.xi-xx), both groups exhibited increased TRAP(+)-staining compared to their counterparts at 6weeks. Increased TRAP(+) staining of osteoclasts, reversal lines, and the extracellular matrix, at the PDL-bone interfaces of mesial furcation, distal, and interradicular regions (Figs.5b.xvi,xviii,xx), was observed compared to controls (Figs.5b.xii,xiv,xix). Of particular interest was the presence of TRAP(+)-stained cells at the coronal regions of the furcation PDL-bone regions (Figs.5b.xv,xvii).

3.5.2. Fiber and nuclei organization—The interdental epithelium exhibited increased width and disorganization in ligated joints compared to controls (Fig.6a). At 6weeks, the congregation of nuclei in the distal apical complex exhibited a more elongated morphology (spindle), increased organization, and sparser distribution in the ligated joint compared to the control joint (Figs.6b.iii,iv). Fiber morphology showed that the crimped morphology of the PDL ligament in controls was lost in areas that experienced elongation of nuclei (Fig. 6b.iv). Interestingly, at 12weeks apical complexes of ligated joints exhibited the characteristics described at 6weeks (Figs.6c.ii,iv). At the PDL-cementum interfaces, nuclei

NIH-PA Author Manuscript

NIH-PA Author Manuscript

NIH-PA Author Manuscript

were organized along the cementum surface in correlation with the advancement of mineralization fronts (Figs.6c.ii,iv). Coronal regions of the viable (non-degraded) complex exhibited similar trends to that observed at apical regions (Fig.S1).

3.5.3. Collagen birefringence—Overall, transseptal fibers in control joints exhibited heavy birefringence while those in ligated joints exhibited decreased and patchy birefringence. No significant differences in collagen birefringence and random fiber directionality were observed at 6weeks (Figs.6b.v-viii,ix-xii) between control and ligated joints. At 12weeks the ligated PDL-cementum interface exhibited increased birefringence (Fig.6c.vi) compared to the rest of the bulk PDL in mesial regions. Birefringence was noticeably thinner next to primary cementum than next to secondary cementum at comparable angles of polarization. When comparing distal complexes, ligated joints showed heavy birefringence in the bulk PDL primarily in coronal regions (Fig.6c.viii) where fibers ran perpendicularly with the cementum and bone compared to oblique fibers in the control (Fig.6c.vii). Apical regions showed high birefringence at distal PDL-cementum interfaces with less birefringence in the bulk PDL.

4. Discussion

In this study, it was hypothesized that periodontitis could change the biomechanical response of the fibrous joint through adaptation. Hence, biomechanical correlates with changes in morphology due to mineralization and resorption will be discussed to highlight the effects of 1) altered joint biomechanics and a 2) subsequent shift in mechanobiology leading to compensatory mechanisms identified as joint adaptation. The fundamental hallmarks of periodontitis that generated coronal biomechanical instability within the ligature model included: crestal bone resorption with a decrease in crestal height (Fig.S2b), deterioration of transseptal fibers with adjacent teeth and of crestal ligament attachment with the tooth (Figs.S2b and 6b,c), and changes in PDL-space (Fig.5a), i.e. functional space from a biomechanical perspective (Lee and Lin et al., 2013). In addition, despite the presence of remaining attachment, i.e. the softer periodontal mechanical “links” between cementum and bone, the gradients in TNF-α expression (Fig.S2c) indicated that the quality of the links could be different from their respective controls. Furthermore, the observed changes in functional space following 6 and 12weeks of ligation, due to resorption and/or growth observed at the PDL-bone and PDL-cementum interfaces, are proposed as a compensatory mechanism – an adaptation in an attempt to maintain joint function – that shifts the organ towards malfunction (Fig.5).

Based on the innate nature of the PDL, during periodontitis, the solid (elastic)-to-fluid (viscous) ratio could change in a manner similar to the effects commonly observed in other biphasic skeletal tissues such as tendons, cartilage, and ligaments (Duenwald-Kuehl et al., 2012; Duenwald et al., 2009; Holmes et al., 1985; Kondratko et al., 2013; LaCroix et al., 2013; Mow et al., 1984). The solid phase includes fibrillar proteins dominated by collagen, various globular proteins, and PGs, which have a semi-solid resemblance. The fluid phase contains water, a combination of interstitial fluid (bound and unbound) and blood, which resides within vessels, and provides nutrients to the complex. Following induction of disease, an observed inevitable biochemical change was increased gradients of TNF-α

NIH-PA Author Manuscript

NIH-PA Author Manuscript

NIH-PA Author Manuscript

expression (Fig.S2c), which is thought to increase matrix metalloproteinase (MMP) activity and thus cause tissue breakdown and decreased bound water retention characteristics of the tissue (Ahn et al., 2013; Nishikawa et al., 2002). Prolonged function and depending on the stage of the disease, plausible effects would be different amounts of solid and fluid, as well as a change in quality of the respective phases and their interactions. Hence, altered biomechanics at 6 and 12weeks of disease progression and their respective controls were evaluated by recording joint response at different loading rates (Supplemental Table 1).

Several biochemical events affect periodontal attachment during disease. These include increased levels of MMPs and RANKL, breakdown of PGs and collagen crosslinks, deterioration of collagen fibrils, and TRAP(+) clastic activity directly related to a change in forms of bone and cementum (Fig.5b) (Ababneh et al., 1999; Giannobile et al., 2003; Lee et al., 2013; Waddington et al., 1998; Waddington et al., 2000). The disease-related outcomes at earlier stages of progression can manifest into changes in form and the quality of tissues within the coronal complex (Lee et al., 2013). Both these aspects within the coronal complex are crucial for resisting joint failure when higher loads at a higher speed are placed on the joint. Based on pure morphological analysis (Figs.S2b and 5a) with all other parameters remaining a constant, it is conceivable that the tooth can displace more into the alveolar socket as illustrated through compression tests (Figs.1c,d) and DIC (Fig.4). With increased degrees of freedom arise an increased displacement resulting in a lower stiffness as observed in the case of diseased joints (Figs.1c,d). An increased change in stiffness between healthy and diseased joints was most seen as the tooth was displaced more into the socket (at higher peak loads) at both time points (Figs.1c,d and 4).

While stiffness provides an insight to the behavior of the diseased joint as it continues to bear higher loads (harder diets), it minimally decouples the load bearing nature due to fluid compartments. Fluids also are an integral part in providing a joint with its innate biomechanical characteristics. Additionally, resistance offered by the fluid can change both due to rate at which the joint is loaded (shear stress to shear strain phenomenon related to viscosity) within and across groups (controls and diseased), and fluid time-related change in interaction of the fluid with the solid fragments as a result of tissue deterioration – a predominant effect in experimental groups. Hence, reactionary load rate at different displacement rates was calculated and load relaxation tests were performed specifically after observing the diverging but increasing reactionary response of the joints at higher displacement rates (equivalent to percent strain) and peak loads in comparison to diseased joints. Trends included a slower reactionary response to loads regardless of rate of loading (Fig.1).

The observed effects of load rate increased with increasing loading velocity (Figs.1a, b, e), which could be correlated to decreased retention of interstitial fluid. Decreased retention of interstitial fluid is speculated due to degradation of transseptal and coronal PDL attachment fibers, decreasing the surface area for bound water and increasing matrix porosity to allow water to flow easily through the organic matrix (Bergomi et al., 2010). As such, hydrostatic pressure observed under control conditions would not be maintained, and the ligated joint in the earlier stages could exhibit a decreased response to load rate as evidenced through our data (Fig.1). The load rate response was best illustrated in this study by recording load

NIH-PA Author Manuscript

NIH-PA Author Manuscript

NIH-PA Author Manuscript

relaxation at two different rates with an order of magnitude difference (0.2 and 2.0mm/min). The joint, regardless of its state, demonstrated increased load relaxation at higher rate of loading when compared to one tenth of loading speed (Fig.2). This effect is best explained by using the classic model of "nonlinear fluid solid interaction during compression (NFSI)" (Holmes et al., 1985; Mow et al., 1984), which highlights the significance of fluid motion through percent solid compaction and its effect on joint response as related to loading rates. Of consequence to this study is the application of the NFSI model to explain the dynamics of the healthy joint and the shift thereof between healthy and diseased joints at two different speeds (0.2 and 2.0mm/min.).

By nature, softer and harder matrices are permeable, and their permeability increases with breakdown of tissues. In parallel, fluid interaction with the solid phase could change, inversely prompting an overall change in organ mechanics. Healthy and diseased joints when loaded at a faster rate behaved closer to pseudoelastic materials, i.e. lower load relaxation when compared to slower rates of loading (Fig.2). This behavior is thought to occur due to increased resistance to fluid motion with the percent compressed solid in case of systems loaded rapidly, prompting them to appear elastic-like (Holmes et al., 1985; Mow et al., 1984). However, given such a scenario, decreased apparent differences in load relaxation (Fig.2) and recovery (Fig.3) responses were identified between healthy and diseased specimens after 6weeks and between diseased specimens after 6 and 12weeks of ligation. Based on the NFSI model, it is here that we speculate that the permeability of PDL in the 6-week diseased specimens was less than that of the PDL in control specimens but could be greater than that of the PDL in 12-week diseased specimens. However, following induction of disease and with the emerging dominance of solid compartment, it is likely that the complex had decreased dampening capability and that the load bearing capacity is limited to lower rates of loading – two effects that are exacerbated after 12weeks. Additionally, it is possible that the fibrous matrix of the ligament did not retain the innate water binding nature and as such contained less bound fluid compared to its healthy and 6-week ligated counterparts. This also implies that elastic recovery could decrease alluding to a decreased ability to absorb higher loads over a shorter period of time (Fig.3b). Interestingly, the difference between healthy and diseased joints decreased with increased time of disease, suggesting that an age-related decrease in fluid flow (e.g. decreased permeability) and matrix changes could have occurred in our animal model (Komatsu et al., 2004).

This study looks at the end result of a compensatory mechanism as a consequence of disease and thus is discussed as an adaptation. Based on results from our previous study (earlier time points of 4, 8, and 15 days) and those in this study (6 and 12weeks), a significant outcome of compensatory mechanism was observed through cementum growth by 15 days and continued to be the same with prolonged disease. Additional outcomes included a change in collagen birefringence and random fiber angulation through 6weeks of ligation (Fig.6b), but also an increased birefringence with a preferential orientation at 12weeks with increased nuclear alignment and elongation, indicating the alignment and stretching of PDL cells (Fig. 6c). These outcomes are time-related compensatory consequences of coronal loss of attachment and an attempt to maintain joint function despite deterioration of softer and

NIH-PA Author Manuscript

NIH-PA Author Manuscript

NIH-PA Author Manuscript

harder constituents due to initial induction of LPS-soaked ligatures (see supplemental section S4).

Disease in general prompts a change in glycosaminoglycan-collagen interactions and, as a result, the interaction of the soft tissue with the interstitial fluid, fixed charge density, stretch capacity of the organic matrix, permeability, and fluid flow-to-solid compaction ratio – all of which aid in load reactionary response of the joint. The effect of fluid drag on load bearing characteristics of joints is largely seen when the joint was loaded at different rates. The two compartment theory of solid-to-fluid ratio plays a significant role in diseased joints. It is challenging to note the change in the ratio of the phases with time; however, by performing load relaxation studies we predict that the solid-to-fluid ratio for the 6-week diseased state was lower compared to that of the 12-week diseased state. This argument is further corroborated with the histological observations of increased matrix compaction by increased birefringence and fiber uncrimping (Fig.6b,c). In response to compression, the greater displacement of the tooth in the socket and lower stiffness of the joint can “potentiate” amplified fiber straining and alignment in response to perpetuating parafunction. The increased expression and altered localization of TRAP show that at 12weeks an increase in compression reminiscent of hyperfunction (Lee et al., 2013; Nozaki et al., 2010; Walker et al., 2008) occurred within furcation and interdental bone (Fig.5b), i.e. the fulcrum about which the tooth is thought to pivot during function (Chattah et al., 2009; Lin et al., 2013; Naveh et al., 2012).

Sustained function on disease and innate physiology related morphological changes are thought to potentiate an altered mechanobiology. An altered mechanobiology could manifest into changes in tissues biomechanics that constitute the complex. The noted change identified by load rate response was in the softer constituent, i.e. the ligament, within which resides solid and fluid compartments. While the degraded coronal regions of the fibrous joint cause increased tooth mobility, the interfacial motion can alter the mechanobiology. As such, the phenotypic expressions of cells at the existing PDL-bone and PDL-cementum, and within the PDL *per se*, can change to that of a fibrous tissue (Brunski, 1999; Wazen et al., 2013). Hence, it is possible that with decreased matrix permeability, solid-to-fluid interaction, and loss in mechanical integrity of the solid compartment, the non-degraded PDL within the apical regions of the diseased complex becomes closer to mimicking conditions of a so called pseudo PDL which is a fibrous tissue that is thought to form due to micromotion between a dental implant and bone (Brunski, 1999; Hori and Lewis, 1982; Lee and Lin et al., 2013; Wazen et al., 2013). As such, past 6 weeks of disease induction, a plausible effect with increased mobility of the tooth is increased collagen turnover leading to a fibrous tissue between bone and cementum layers with minimal dampening characteristics and an increased risk of hard tissue fracture that constitute the organ.

5. Conclusion

Periodontitis shifted the biomechanics of the joint toward properties reflective of increased joint mobility (Fig.7a). An altered PDL-space, shifts in expression levels and localization of TRAP(+) staining, and advancement of mineralization fronts in secondary cementum, highlighted the possibility of strain amplification within the diseased joint. Because

NIH-PA Author Manuscript

NIH-PA Author Manuscript

NIH-PA Author Manuscript

increased mobility due to decreased bone-PDL-tooth attachment generated adaptive effects, the joint could be potentiated towards failure by positive feedback. An additive effect is created through alterations to the soft tissue constituents of the joint through shifts in the PDL fiber morphology to an increasingly fibrous characteristic (Fig.7b). Decreased load relaxation and recovery curves hinted on decreased permeability of the organic matrix, allowing increased fluid drag (Fig.7b) and decreased dampening characteristics. From an applied science perspective, diseased joints could be at an increased failure risk for a given load when compared to its healthy counterpart. From a clinical perspective, it is proposed that a patient affected by periodontitis should refrain from a hard diet (i.e. high load response) as well as hard and/or quick chewing motions (i.e. high displacement rate and/or high loads).

Supplementary Material

Refer to Web version on PubMed Central for supplementary material.

Acknowledgments

The authors also thank the Biomaterials and Bioengineering Micro-CT Imaging Facility at UCSF for the use of the Micro-XCT unit and the *in situ* loading device. Support was provided by NIH/NIDCR R00DE018212 (SPH), NIH/NIDCR R01DE022032(SPH), NIH/NIDCR T32DE07306-16(JDL), NIH/NCRR S10RR026645(SPH), and the Department of Preventive and Restorative Dental Sciences, UCSF, and the Department of Orofacial Sciences, UCSF.

References

Ababneh KT, Hall RC, Embery G. The proteoglycans of human cementum: immunohistochemical localization in healthy, periodontally involved and ageing teeth. Journal of periodontal research. 1999; 34:87–96. [PubMed: 10207837]

Ahn SJ, Rhim EM, Kim JY, Kim KH, Lee HW, Kim EC, Park SH. Tumor Necrosis Factor-Alpha Induces Matrix Metalloproteinases-3, -10 and -13 in Human Periodontal Ligament Cells. Journal of periodontology. 2013 (doi:10.1902/jop.2013.130063).

Alexopoulos LG, Williams GM, Upton ML, Setton LA, Guilak F. Osteoarthritic changes in the biphasic mechanical properties of the chondrocyte pericellular matrix in articular cartilage. Journal of biomechanics. 2005; 38:509–517. [PubMed: 15652549]

Bartold, PM. Bone and tooth interface: periodontal ligament. In: McCauley, LK.; Somerman, MJ., editors. Mineralized Tissues in Oral and Craniofacial Science: Biological Principles and Clinical Correlates. 1. Vol. 227. A John Wiley & Sons, Inc.; 2012.

Beertsen W, McCulloch CA, Sodek J. The periodontal ligament: a unique, multifunctional connective tissue. Periodontology 2000. 1997; 13:20–40. [PubMed: 9567922]

Bergomi M, Cugnoni J, Botsis J, Belser UC, Anselm Wiskott HW. The role of the fluid phase in the viscous response of bovine periodontal ligament. Journal of biomechanics. 2010; 43:1146–1152. [PubMed: 20185135]

Brunski JB. In vivo bone response to biomechanical loading at the bone/dental-implant interface. Advances in dental research. 1999; 13:99–119. [PubMed: 11276755]

Carter, DR.; Beaupré, GS. Skeletal function and form: mechanobiology of skeletal development, aging, and regeneration. Cambridge University Press; 2001.

Chattah NLT, Shahar R, Weiner S. Design strategy of minipig molars using electronic speckle pattern interferometry: comparison of deformation under load between the tooth-mandible complex and the isolated tooth. Advanced Materials. 2009; 21:413–418.

Chen CS, Ingber DE. Tensegrity and mechanoregulation: from skeleton to cytoskeleton. Osteoarthritis and cartilage/OARS, Osteoarthritis Research Society. 1999; 7:81–94.

NIH-PA Author Manuscript

NIH-PA Author Manuscript

NIH-PA Author Manuscript

Dasanayake AP. Periodontal disease is related to local and systemic mediators of inflammation. The journal of evidence-based dental practice. 2010; 10:246–247. [PubMed: 21093812]

Doyle CJ, Bartold PM. How does stress influence periodontitis? Journal of the International Academy of Periodontology. 2012; 14:42–49. [PubMed: 22799128]

Duenwald-Kuehl S, Kondratko J, Lakes RS, Vanderby R Jr. Damage mechanics of porcine flexor tendon: mechanical evaluation and modeling. Annals of biomedical engineering. 2012; 40:1692–1707. [PubMed: 22399329]

Duenwald SE, Vanderby R Jr, Lakes RS. Viscoelastic relaxation and recovery of tendon. Annals of biomedical engineering. 2009; 37:1131–1140. [PubMed: 19353269]

Duenwald SE, Vanderby R Jr, Lakes RS. Stress relaxation and recovery in tendon and ligament: experiment and modeling. Biorheology. 2010; 47:1–14. [PubMed: 20448294]

Fung, YC. Biomechanics: Mechanical Properties of Living Tissues. 2. Springer-Verlag New York, Inc.; New York, New York: 1993.

Giannobile WV, Al-Shammari KF, Sarment DP. Matrix molecules and growth factors as indicators of periodontal disease activity. Periodontology 2000. 2003; 31:125–134. [PubMed: 12656999]

Guilak F, Ratcliffe A, Lane N, Rosenwasser MP, Mow VC. Mechanical and biochemical changes in the superficial zone of articular cartilage in canine experimental osteoarthritis. Journal of orthopaedic research: official publication of the Orthopaedic Research Society. 1994; 12:474–484. [PubMed: 8064478]

Herring, SW. Biomechanics of teeth in bone: function, movement, and prosthetic rehabilitation. In: McCauley, LK.; Somerman, MJ., editors. Mineralized Tissues in Oral and Craniofacial Science Biological Principles and Clincal Correlates. 1. A John Wiley & Sons, Inc.; 2012.

Hiiemae K. Mechanisms of food reduction, transport and deglutition: how the texture of food affects feeding behavior. Journal of Texture Studies. 2004; 35:171–200.

Holmes MH, Lai WM, Mow VC. Singular perturbation analysis of the nonlinear, flow-dependent compressive stress relaxation behavior of articular cartilage. Journal of biomechanical engineering. 1985; 107:206–218. [PubMed: 4046561]

Hori RY, Lewis JL. Mechanical properties of the fibrous tissue found at the bone-cement interface following total joint replacement. Journal of biomedical materials research. 1982; 16:911–927. [PubMed: 7174716]

Hurng JM, Kurylo MP, Marshall GW, Webb SM, Ryder MI, Ho SP. Discontinuities in the human bone-PDL-cementum complex. Biomaterials. 2011; 32:7106–7117. [PubMed: 21774982]

Ingber DE. Mechanobiology and diseases of mechanotransduction. Annals of medicine. 2003; 35:564–577. [PubMed: 14708967]

Ingber DE. Tissue adaptation to mechanical forces in healthy, injured and aging tissues. Scandinavian journal of medicine & science in sports. 2005; 15:199–201. [PubMed: 15998336]

Ingber DE. Cellular mechanotransduction: putting all the pieces together again. The FASEB journal: official publication of the Federation of American Societies for Experimental Biology. 2006; 20:811–827.

Kinney JS, Ramseier CA, Giannobile WV. Oral fluid-based biomarkers of alveolar bone loss in periodontitis. Annals of the New York Academy of Sciences. 2007; 1098:230–251. [PubMed: 17435132]

Komatsu K, Kanazashi M, Shimada A, Shibata T, Viidik A, Chiba M. Effects of age on the stress-strain and stress-relaxation properties of the rat molar periodontal ligament. Archives of oral biology. 2004; 49:817–824. [PubMed: 15308426]

Kondratko J, Duenwald-Kuehl S, Lakes R, Vanderby R Jr. Mechanical compromise of partially lacerated flexor tendons. Journal of biomechanical engineering. 2013; 135:011001. [PubMed: 23363212]

LaCroix AS, Duenwald-Kuehl SE, Brickson S, Akins TL, Diffee G, Aiken J, Vanderby R Jr, Lakes RS. Effect of age and exercise on the viscoelastic properties of rat tail tendon. Annals of biomedical engineering. 2013; 41:1120–1128. [PubMed: 23549897]

Lee JH, Lin JD, Fong JI, Ryder MI, Ho SP. The Adaptive Nature of the Bone-Periodontal Ligament-Cementum Complex in a Ligature-Induced Periodontitis Rat Model. BioMed Research International. 2013; 2013:17.

NIH-PA Author Manuscript

NIH-PA Author Manuscript

NIH-PA Author Manuscript

Lin JD, Aloni S, Altoe V, Webb SM, Ryder MI, Ho SP. Elastic discontinuity and ectopic calcification in a human Q2 cementum–dentin complex. Acta Biomaterialia. 2013; 9(1):4787–4795. [PubMed: 22917805]

Lin JD, Ozcoban H, Greene JP, Jang AT, Djomehri SI, Fahey KP, Hunter LL, Schneider GA, Ho SP. Biomechanics of a bone-periodontal ligament-tooth fibrous joint. Journal of biomechanics. 2013; 46:443–449. [PubMed: 23219279]

Mow VC, Holmes MH, Lai WM. Fluid transport and mechanical properties of articular cartilage: a review. Journal of biomechanics. 1984; 17:377–394. [PubMed: 6376512]

Naveh GR, Lev-Tov Chattah N, Zaslansky P, Shahar R, Weiner S. Tooth-PDL-bone complex: response to compressive loads encountered during mastication - a review. Archives of oral biology. 2012; 57:1575–1584. [PubMed: 22877793]

Nies M, Ro JY. Bite force measurement in awake rats. Brain research. Brain research protocols. 2004; 12:180–185. [PubMed: 15013469]

Nishikawa M, Yamaguchi Y, Yoshitake K, Saeki Y. Effects of TNFalpha and prostaglandin E2 on the expression of MMPs in human periodontal ligament fibroblasts. Journal of periodontal research. 2002; 37:167–176. [PubMed: 12113550]

Nozaki K, Kaku M, Yamashita Y, Yamauchi M, Miura H. Effect of cyclic mechanical loading on osteoclast recruitment in periodontal tissue. Journal of periodontal research. 2010; 45:8–15. [PubMed: 19602121]

Popowics T, Yeh K, Rafferty K, Herring S. Functional cues in the development of osseous tooth support in the pig, Sus scrofa. Journal of biomechanics. 2009; 42:1961–1966. [PubMed: 19501361]

Ten Cate, R. Oral histology: development, structure, and function. Mosby-Year Book, Inc.; 1998.

Thomas NR, Peyton SC. An electromyographic study of mastication in the freely-moving rat. Archives of oral biology. 1983; 28:939–945. [PubMed: 6580850]

Waddington RJ, Embery G, Smith AJ. Immunochemical detection of the proteoglycans decorin and biglycan in human gingival crevicular fluid from sites of advanced periodontitis. Archives of oral biology. 1998; 43:287–295. [PubMed: 9839704]

Waddington RJ, Moseley R, Embery G. Reactive oxygen species: a potential role in the pathogenesis of periodontal diseases. Oral Dis. 2000; 6:138–151. [PubMed: 10822357]

Walker CG, Ito Y, Dangaria S, Luan X, Diekwisch TG. RANKL, osteopontin, and osteoclast homeostasis in a hyperocclusion mouse model. European journal of oral sciences. 2008; 116:312–318. [PubMed: 18705798]

Wazen RM, Currey JA, Guo H, Brunski JB, Helms JA, Nanci A. Micromotion-induced strain fields influence early stages of repair at bone-implant interfaces. Acta biomaterialia. 2013; 9:6663–6674. [PubMed: 23337705]

NIH-PA Author Manuscript
NIH-PA Author Manuscript
NIH-PA Author Manuscript

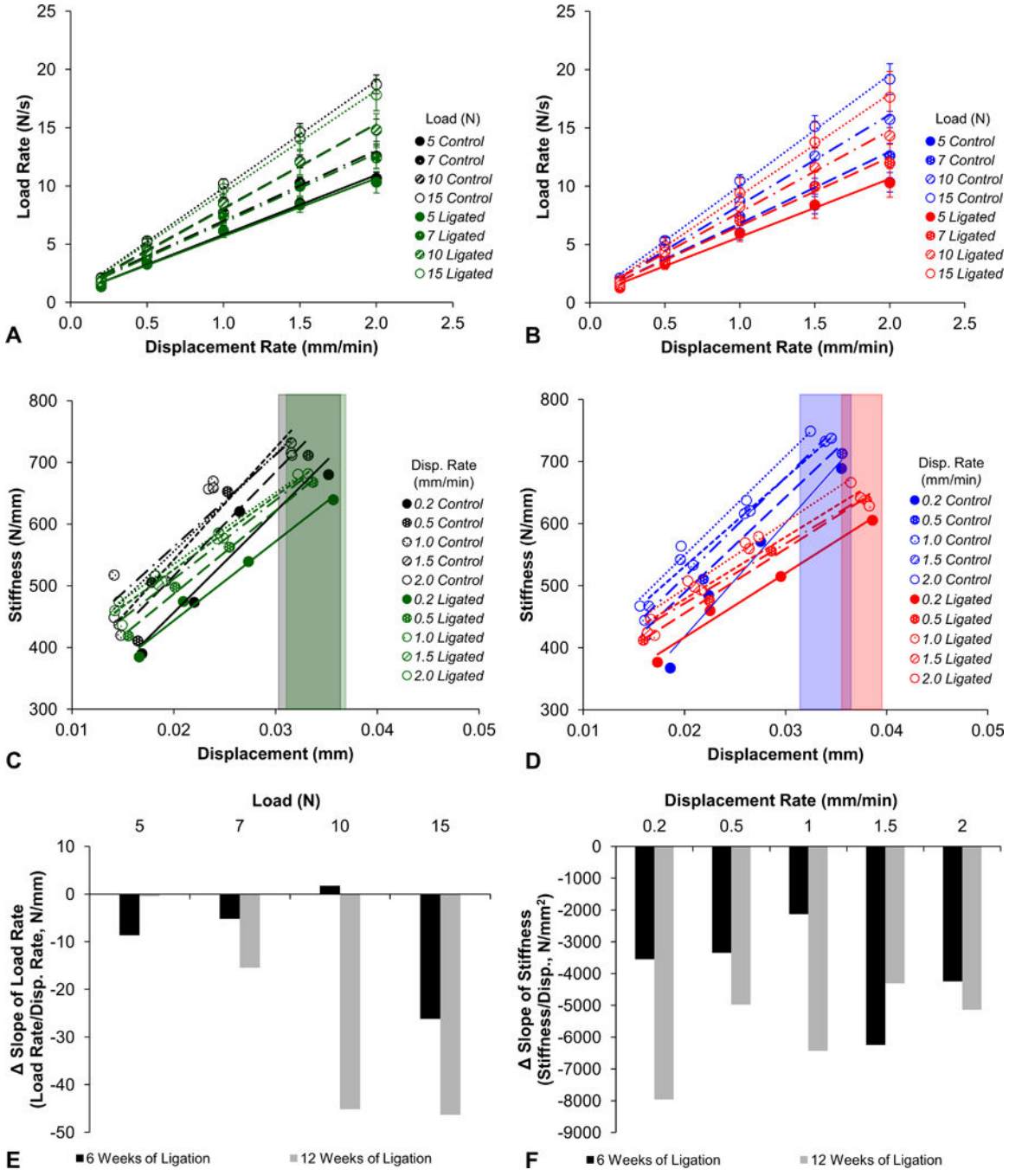

Figure 1. Biomechanical response to simulated cyclical physiological loads

Load rate versus displacement rate plots compare the reactionary load rate response of fibrous joints after 6 weeks *(A; control – black, ligated – green)* and 12 weeks *(B; control – blue, ligated – red)* of ligation. Linear trend lines are fitted through each group of data points from each reactionary peak load using the least squares method. Stiffness versus displacement plots compare the stiffness response of fibrous joints after 6 weeks *(C; control – black, ligated – green)* and 12 weeks *(D; control – blue, ligated – red)* of ligation. Trend lines are plotted through each group of data point from each displacement rate. Color-coded

NIH-PA Author Manuscript

NIH-PA Author Manuscript

NIH-PA Author Manuscript

boxes highlight the differences in displacement ranges between control and ligated groups. Column plots were used to illustrate the differences in slopes between control and ligated groups (control value subtracted from ligated value) at each time point *(6-week – black, 12-week – gray)* as measured from load rate-displacement rate *(E)* and stiffness-displacement *(F)* graphs. *Disp. – displacement.*

NIH-PA Author Manuscript

NIH-PA Author Manuscript

NIH-PA Author Manuscript

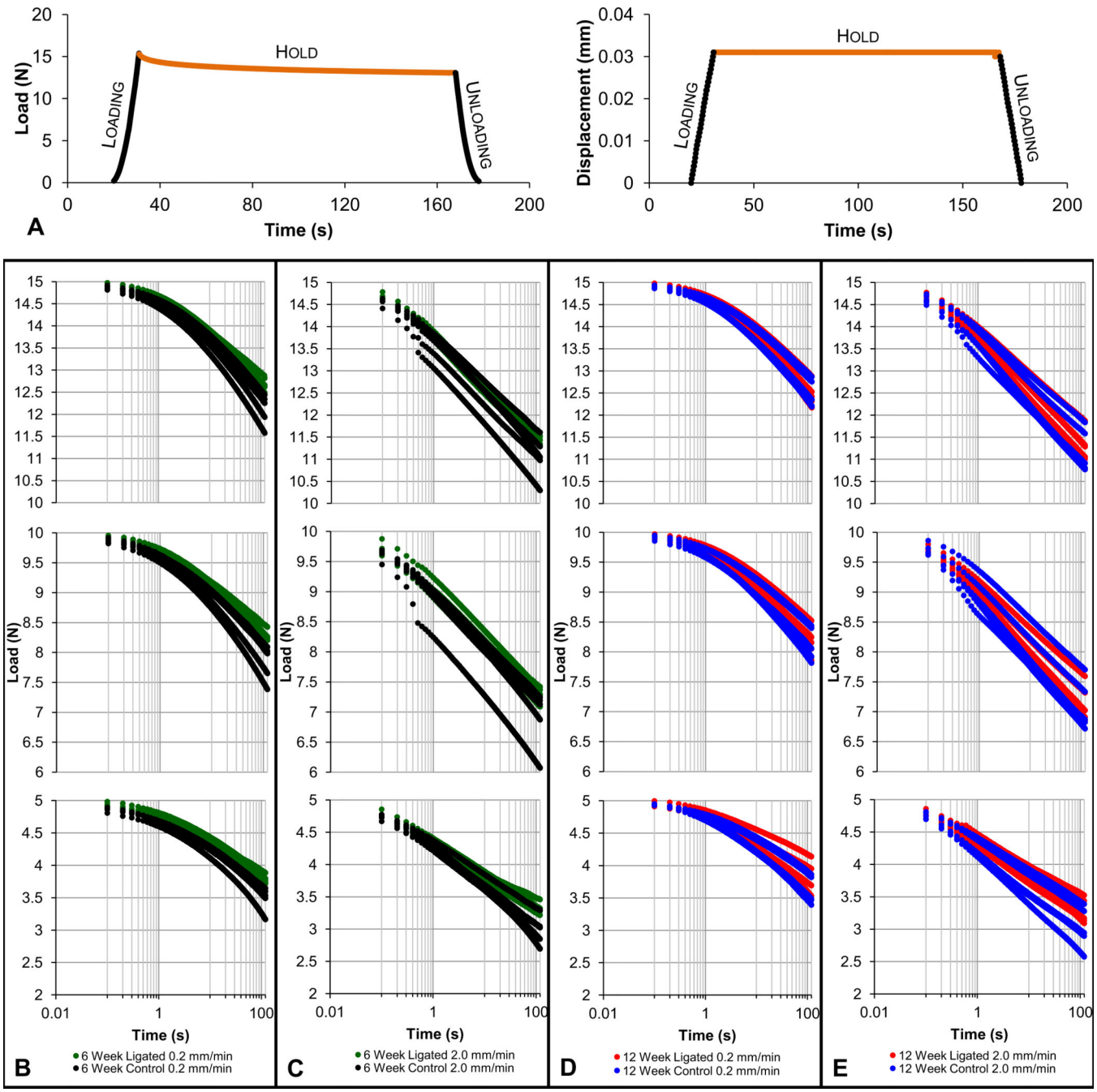

Figure 2. Load relaxation response under constant displacement

(A) Representative load versus time and corresponding displacement versus time plots illustrate the typical loading, hold, and unloading phases of each loading cycle. The hold phase used for load relaxation analysis, during which the displacement is held constant, is highlighted in orange. Load relaxation profiles compare control and ligated fibrous joints that underwent loading at 0.2mm/min *(B)* and 2.0mm/min *(C)* at the 6-week time point and 0.2mm/min *(D)* and 2.0mm/min *(E)* at the 12-week time point. Time values are plotted in logarithmic scale of base 10. Curves are offset for effective comparisons between control and ligated groups at each reactionary peak load. As such, the top row of graphs represents

NIH-PA Author Manuscript

NIH-PA Author Manuscript

NIH-PA Author Manuscript

the hold phase of cycles loaded to a reactionary peak load of 15N, the second row represents those loaded to 10N, and the final row represents those loaded to 5N. *6-week control – black; 6-week ligated – green; 12-week control – blue; 12-week ligated – red.*

NIH-PA Author Manuscript
NIH-PA Author Manuscript
NIH-PA Author Manuscript

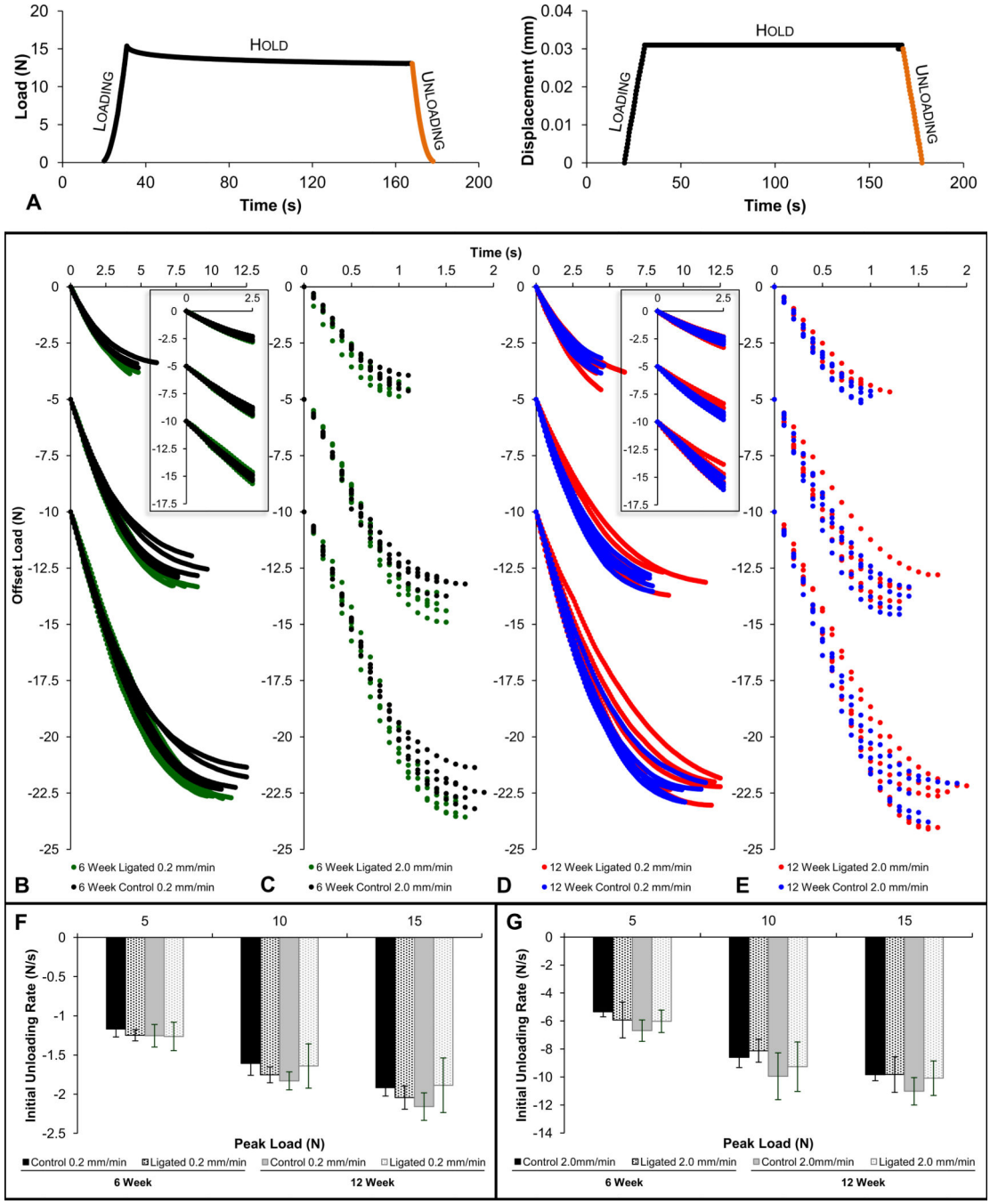

Figure 3. Load recovery response during unloading

(A) Representative load versus time and corresponding displacement versus time plots illustrate the typical loading, hold, and unloading phases of each loading cycle. The unloading phase used for load recovery analysis is highlighted in orange. Load recovery profiles compare control and ligated fibrous joints that underwent loading at 0.2mm/min *(B)* and 2.0mm/min *(C)* at the 6-week time point and 0.2mm/min *(D)* and 2.0mm/min *(E)* at the 12-week time point. Curves were offset to for effective comparisons between control and ligated groups at each reactionary peak load. For each individual graph, the set of curves

NIH-PA Author Manuscript

NIH-PA Author Manuscript

NIH-PA Author Manuscript

decreasing from 0N represents the unloading phase of cycles loaded to a reactionary peak load of 5N, the set of curves decreasing from −5N represents those loaded to 10N, and the final set of curves decreasing from −10N represents those loaded to 15N. Equivalent column plots compare initial unloading load rates at 0.2mm/min *(F)* and 2.0mm/min *(G)* of unloading between control *(solid)* and ligated *(dotted)* fibrous joints after 6 weeks *(black)* and 12 weeks *(gray)* of ligation. *(B-E) 6-week control – black; 6-week ligated – green; 12-week control – blue; 12-week ligated – red.*

NIH-PA Author Manuscript
NIH-PA Author Manuscript
NIH-PA Author Manuscript

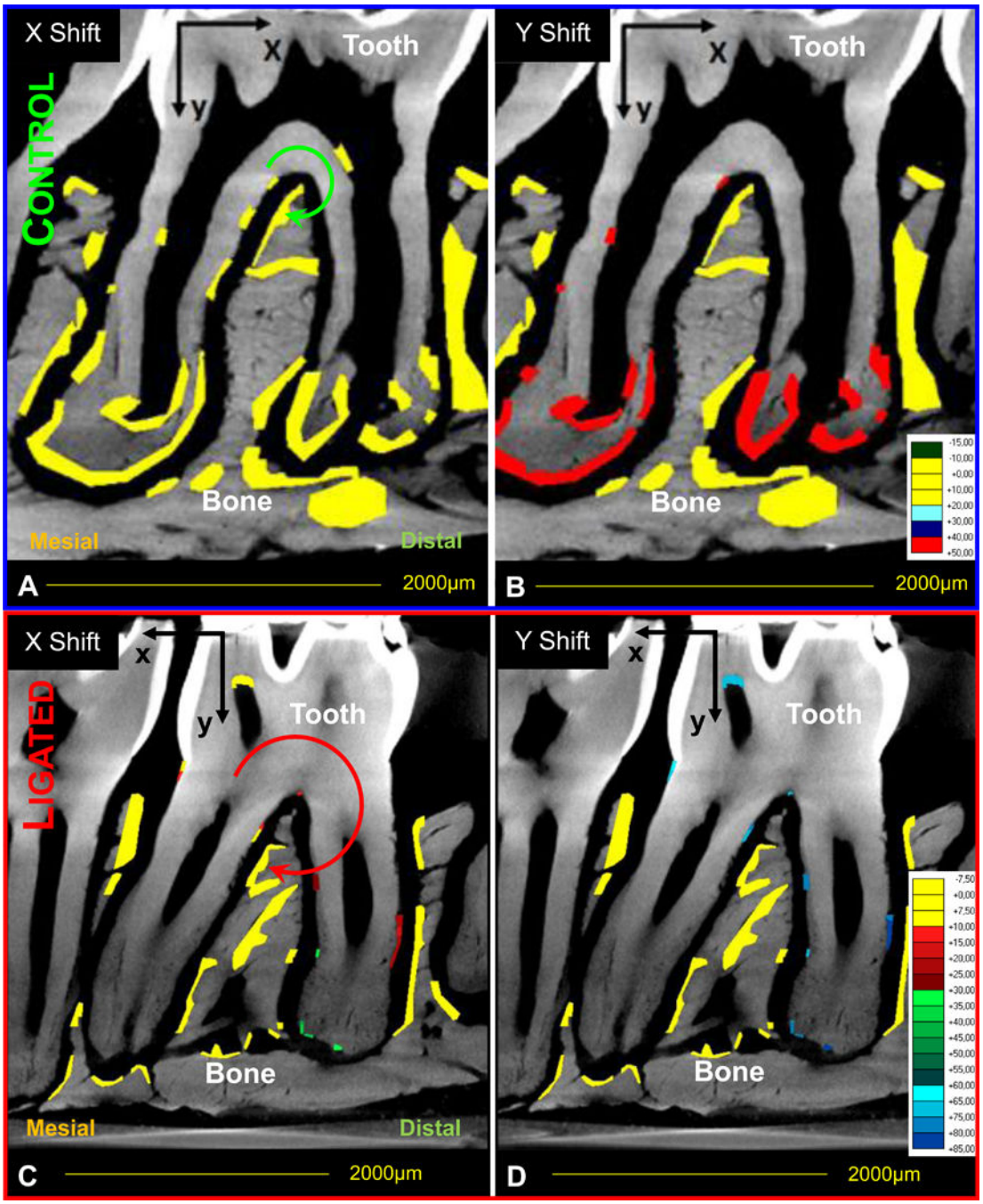

Figure 4. Calculated tooth displacement within the alveolar bone socket using digital image correlation (DIC)

Comparisons in tooth displacement relative to the bone within control *(A,B)* and ligated *(C,D)* joints. Color-coded regions indicate areas analyzed for changes in horizontal (X-axis, *A, C*) and vertical (Y-axis, *B, D*) displacement fields. Each color represents a different displacement range. Please note the axis and displacement range changes for displacement vectors between control and ligated joints. Circular arrows are representative (not to scale) indicators of the direction and magnitude of tooth movement based on calculated DIC values.

NIH-PA Author Manuscript
NIH-PA Author Manuscript
NIH-PA Author Manuscript

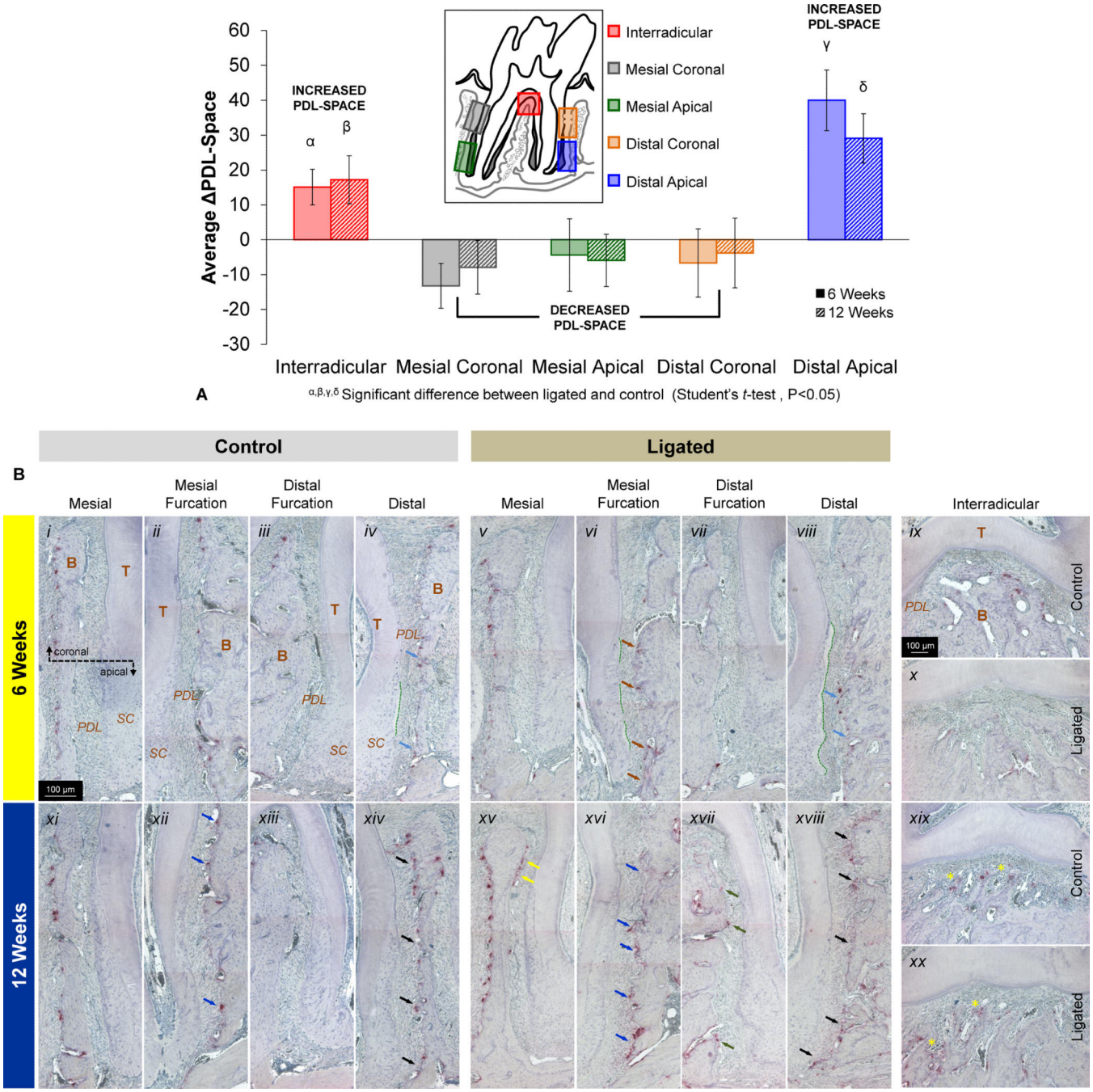

Figure 5. Correlation between morphometrics and osteoclastic activity as analyzed through PDL-width and TRAP staining

(A) The column graph shows differences in average PDL-space measurements between control and ligated fibrous joints (control values subtracted from ligated values) at interradicular *(red)*, mesial coronal *(grey)*, mesial apical *(green)*, distal coronal *(orange)*, and distal apical *(blue)* regions. Both 6-week *(solid)* and 12-week *(hashed)* time points are plotted. Positive values indicate increased PDL-space in ligated joints compared to controls while negative values indicate decreased PDL-space in ligated joints compared to controls. $^{\alpha, \beta, \gamma, \delta}$ Significant difference between ligated and control within each region

NIH-PA Author Manuscript

NIH-PA Author Manuscript

NIH-PA Author Manuscript

(Student's *t-test, P<0.05*). *(B)* Light micrograph images taken at 10× magnification compare localization and intensity of TRAP(+) staining within osteoclasts, reversal lines, and the extracellular matrix of control *(i-iv, ix, xi-xiv, xix)* and ligated *(v-viii, x, xv-viii, xx)* joints after 6 weeks *(i-x)* and 12 weeks *(xi-xx)* of ligation. At 6 weeks, differences are annotated in distal *(light blue arrows)* and mesial furcation *(brown arrows)*. At 12 weeks, differences are noted in mesial *(yellow arrows)*, mesial furcation *(blue arrows)*, distal furcation *(green arrows)*, and distal regions *(black arrows)* are compared. Advancement of secondary cementum is also highlighted *(green hashed lines)*. Please note that tissues within each image were oriented similarly based on corresponding regions of mesial coronal, mesial apical, distal coronal, distal apical, and interradicular. *T – tooth; B – bone; PDL – periodontal ligament; SC – secondary cementum.*

NIH-PA Author Manuscript
NIH-PA Author Manuscript
NIH-PA Author Manuscript

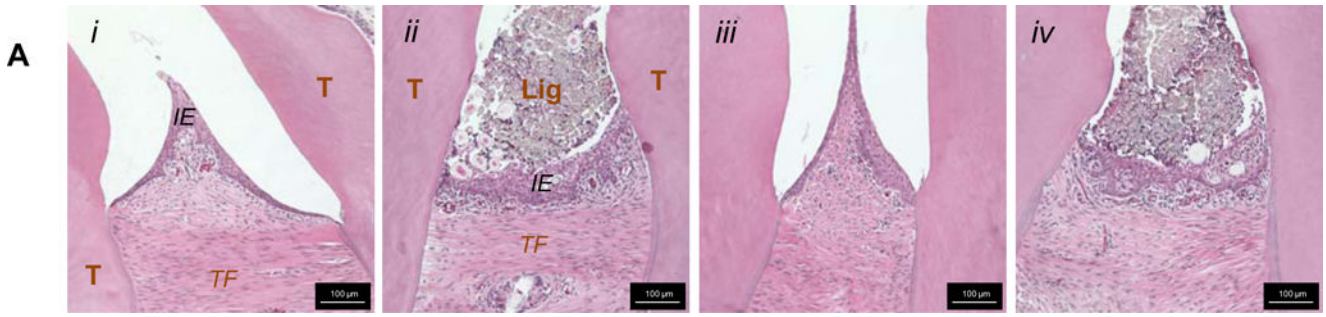

NIH-PA Author Manuscript
NIH-PA Author Manuscript
NIH-PA Author Manuscript

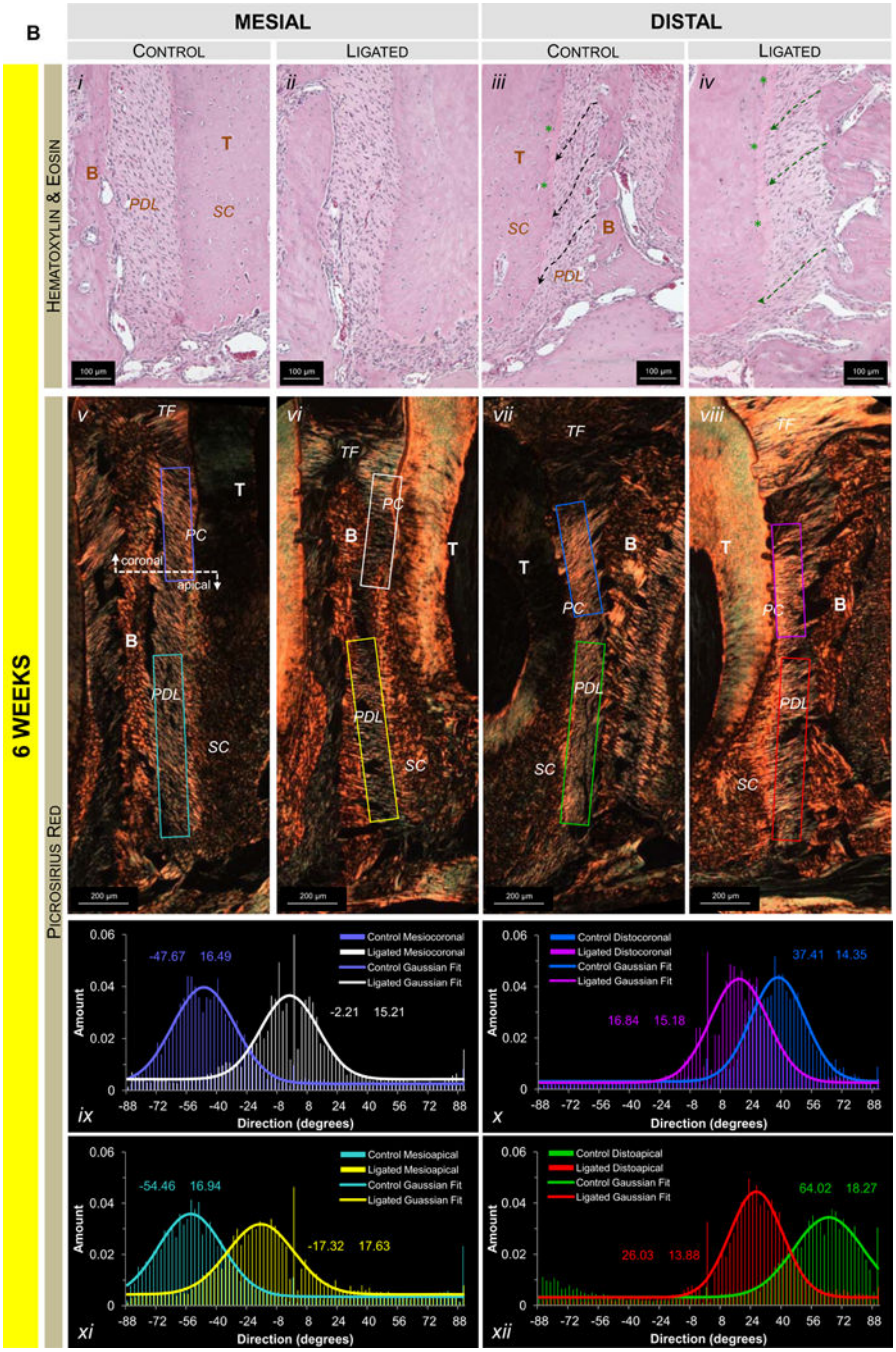

NIH-PA Author Manuscript
NIH-PA Author Manuscript
NIH-PA Author Manuscript

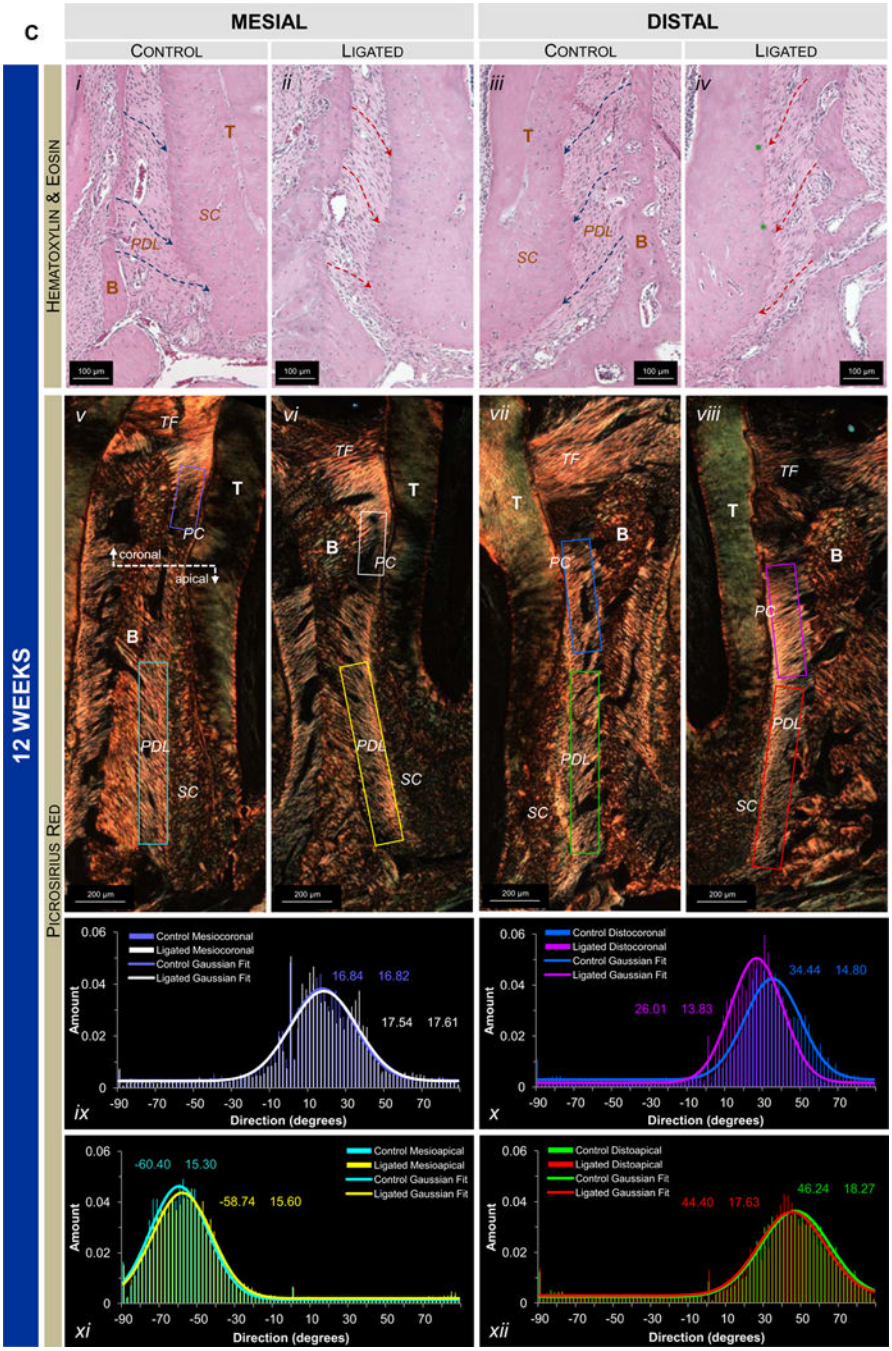

Figure 6. Histological observations of collagen fiber orientation, shape, and organization

(A) Representative H&E-stained sections at 10× magnification show interproximal gingiva adjacent to the second molar of 6-week control *(i)*, 6-week ligated *(ii)*, 12-week control *(iii)*, and 12-week ligated *(iv)* rats. Representative micrographs of corresponding H&E-stained (10× magnification; *B.i-iv, C.i-iv)* and PSR-stained (4× magnification; *B.v-viii, C.v-viii)* sections compare differences in the apical mesial and distal regions of control and ligated fibrous joints at 6-week *(B)* and 12-week *(C)* time points. *(B.i-iv, C.i-iv)* Differences in morphology of nuclei *(along hashed arrows)* and advancement of the mineralization front

NIH-PA Author Manuscript

NIH-PA Author Manuscript

NIH-PA Author Manuscript

(green asterisks) are highlighted. *(B.v-viii, C.v-viii)* Images of PSR-stained sections were taken using polarized light. Plots illustrate directionality of birefringent collagen fibers within mesial apical *(B.ix, C.ix)*, distal coronal *(B.x, C.x)*, and distal apical regions *(B.xi, C.xi)*. Color coding within plots correspond to colored boxes within micrographs. *T – tooth; IE – interdental epithelium; TF – transseptal fibers; Lig – ligature; B – bone; PDL – periodontal ligament; SC – secondary cementum.*

NIH-PA Author Manuscript

NIH-PA Author Manuscript

NIH-PA Author Manuscript

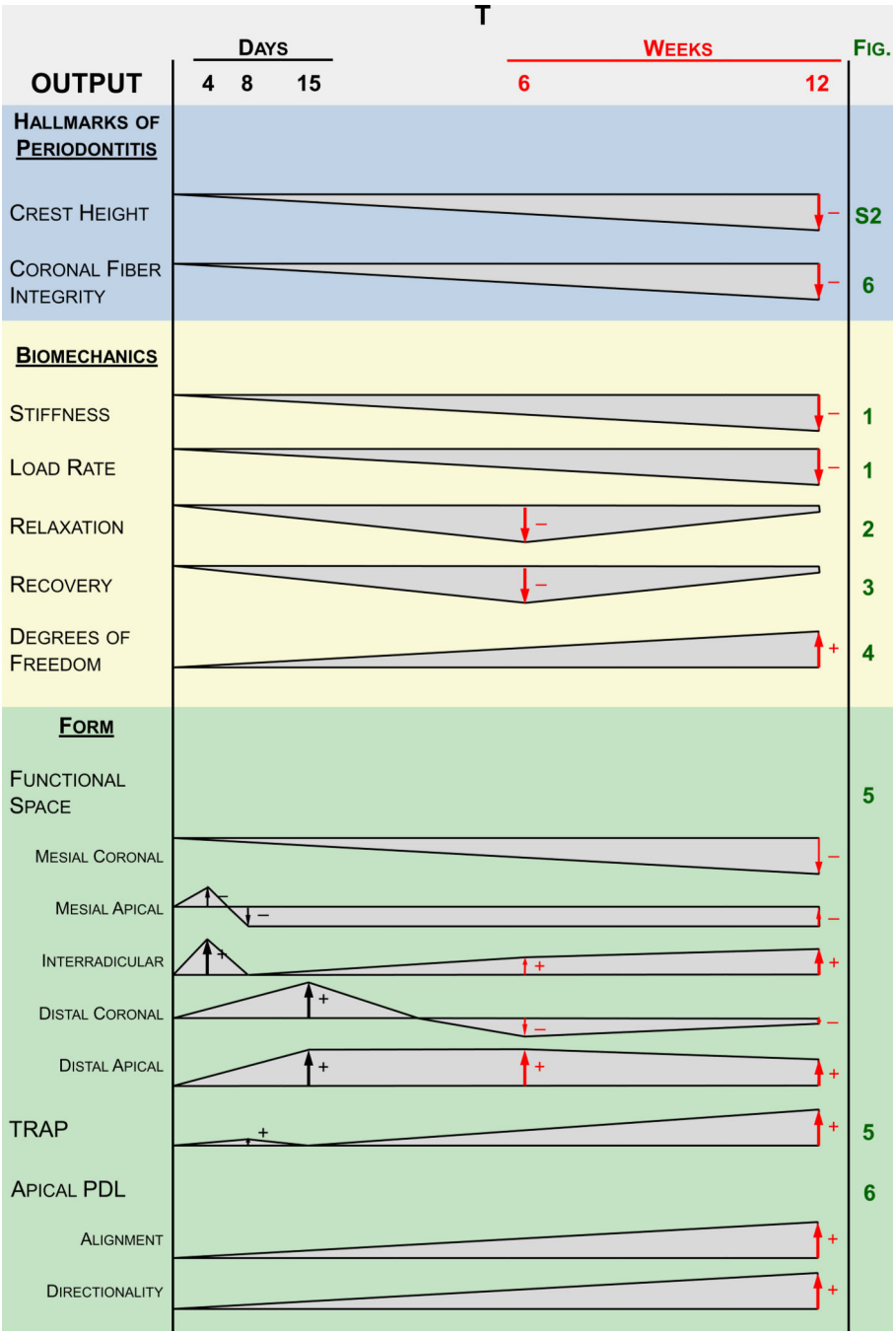

NIH-PA Author Manuscript

NIH-PA Author Manuscript

NIH-PA Author Manuscript

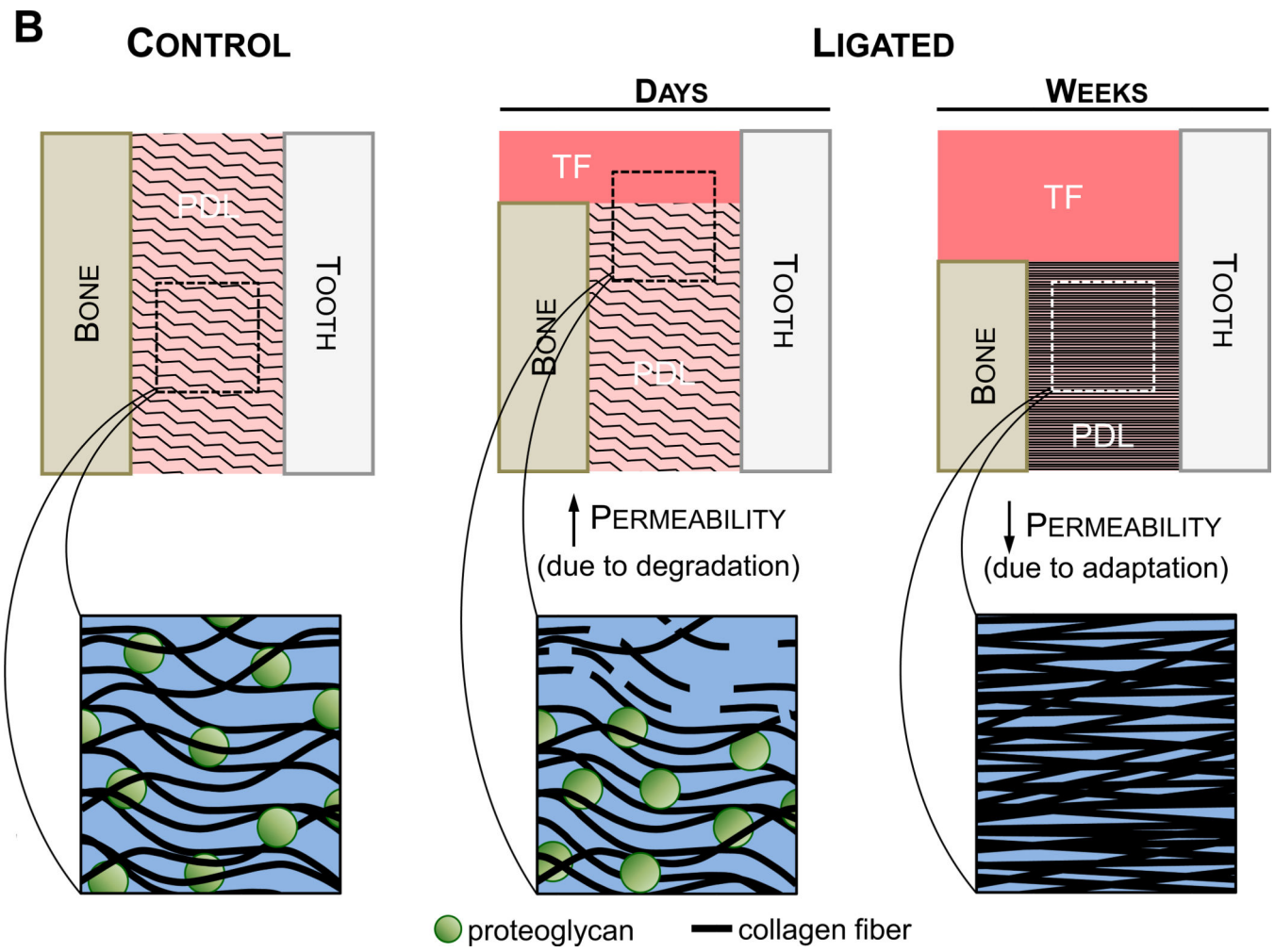

Figure 7. Suggested model summarizing the findings in a temporal fashion

(A) These observations are based on the hallmarks of periodontitis, joint biomechanics, and morphological features of the soft tissue and the overall joint. Polygonal shapes illustrate deviation of the diseased joint from the control joint based on magnitude. The negligible differences at the beginning of the timeline represent no differences in baseline measurements between the two groups at the start of ligation. Arrows represent the increase and/or decrease in deviation. *(B)* Illustrations showing the suggested differences in permeability that correlate to the findings at both the early stages (4-15 days) (Lee and Lin et al., 2013) and later stages (6-12 weeks) of the study. Permeability to fluid flux is expected to increase during the initial degradative phase of the disease, during which the host response to inflammation causes degeneration of transseptal fibers and a decrease in crestal bone height. Strain-induced adaptation due to the increased mobility of the tooth is observed within the apical regions of the PDL at later stages of periodontitis, leading to increased fibrous tissue formation and a decrease in proteoglycan content. Permeability of the tissue is decreased leading to a decrease in load relaxation and load recovery characteristics in the diseased fibrous joint at a later stage. As such, the cause of decreased stiffness and load rate is attributed to a loss in PDL attachment and degradation of the coronal aspects of the joint, while the decrease in load relaxation (at higher loads) and recoverability (at lower loads) can

NIH-PA Author Manuscript

NIH-PA Author Manuscript

NIH-PA Author Manuscript

be attributed to adaptation of the joint. Please note that the observed biomechanically-induced adaptations outlined in this model are reserved to the soft tissue elements of the fibrous joint.